PHYSICAL REVIEW C **71**, 044307 (2005)

Radiative strength functions in $^{93-98}$Mo

M. Guttormsen,[1,*] R. Chankova,[1] U. Agvaanluvsan,[2] E. Algin,[2,3,4,5] L. A. Bernstein,[2] F. Ingebretsen,[1] T. Lönnroth,[6] S. Messelt,[1] G. E. Mitchell,[3,4] J. Rekstad,[1] A. Schiller,[2] S. Siem,[1] A. C. Sunde,[1] A. Voinov,[7,8] and S. Ødegård[1]

[1]*Department of Physics, University of Oslo, N-0316 Oslo, Norway*
[2]*Lawrence Livermore National Laboratory, L-414, 7000 East Avenue, Livermore, California 94551*
[3]*North Carolina State University, Raleigh, North Carolina 27695*
[4]*Triangle Universities Nuclear Laboratory, Durham, North Carolina 27708*
[5]*Department of Physics, Osmangazi University, Meselik, Eskisehir, 26480 Turkey*
[6]*Department of Physics, Åbo Akademi, FIN-20500 Turku, Finland*
[7]*Department of Physics and Astronomy, Ohio University, Athens, Ohio 45701*
[8]*Frank Laboratory of Neutron Physics, Joint Institute of Nuclear Research, 141980 Dubna, Moscow Region, Russia*

(Received 26 November 2004; published 20 April 2005)

Radiative strength functions (RSFs) in $^{93-98}$Mo have been extracted using the (^{3}He,$\alpha\gamma$) and (^{3}He,^{3}He$'\gamma$) reactions. The RSFs are U shaped as function of γ energy with a minimum at around $E_\gamma = 3$ MeV. The minimum values increase with neutron number because of the increase in the low-energy tail of the giant electric dipole resonance with nuclear deformation. The unexpected strong increase in strength below $E_\gamma = 3$ MeV, here called soft pole, is established for all $^{93-98}$Mo isotopes. The soft pole is present at all initial excitation energies in the 5−8-MeV region.

DOI: 10.1103/PhysRevC.71.044307 PACS number(s): 24.30.Gd, 24.10.Pa, 25.55.Hp, 27.60.+j

I. INTRODUCTION

The γ decay of nuclei at high excitation energy tends to follow certain statistical rules. The dominating γ-transition driving factors are the number of accessible final states and the γ-ray transmission coefficient. The largest uncertainties are connected to the latter factor. In the description of this factor Blatt and Weisskopf [1] included an E_γ^{2L+1} dependency, where L is the angular momentum transfer in the transition. In their definition of the radiative strength function (RSF), this simple energy dependence was divided out. With such a definition, the single-particle RSF (Weisskopf) estimates become independent of γ-ray energy. Various concepts of RSFs and γ decay in the continuum are outlined in the reviews of Bartholomew *et al*. [2,3].

It has been well known that the RSF is not at all constant but shows an additional E_γ^x dependency with $x = 1-2$ for γ energies in the 4−8-MeV region. Axel [4] argued that this feature is because of the collective giant electric dipole resonance (GEDR), which represents the essential mechanism for the γ decay. However, the situation is more complex. Further studies [5–7] reveal fine structures in the RSF, which are commonly called pygmy resonances. This name does not refer to specific structures: the $E1$ pygmy resonance in the $E_\gamma = 5-7$ MeV region of gold to lead nuclei could be because of neutron skin oscillations [8], whereas bumps in the 3-MeV region of rare earth nuclei are now determined to be of $M1$ character [9,10]. The electromagnetic character and measured strength of the latter pygmy resonance is compatible with the scissors mode [11]. Recently [12,13], the RSF picture of iron isotopes has been further modified by the observation of an anomalous increase in strength at γ energies below 4 MeV. It is clear that in the present situation, new experimental results are urgently needed.

The stable molybdenum isotopes are well suited as targets for the study of nuclear properties when going from spherical to deformed shapes. In this work we perform a systematic analysis of the RSFs of the six $^{93-98}$Mo isotopes. The RSFs depend on the dynamic properties of electric charges present within these systems ($Z = 42$). Because the nuclear deformation varies from spherical shapes ($\beta \sim 0$) at $N = 51$ to deformed shapes ($\beta \sim 0.2$) at $N = 56$, we expect to observe effects because of shape changes. Furthermore, these nuclei reveal weak GEDR tails at low E_γ, making them interesting objects in the search for other weak structures in the RSF.

The Oslo Cyclotron group has developed a sensitive tool to investigate RSFs for E_γ below the neutron binding energy S_n. The method is based on the extraction of primary γ-ray spectra at various initial excitation energies E_i measured in particle reactions with one and only one charged ejectile. From such a set of primary γ spectra, nuclear level densities and RSFs can be extracted [14–16]. The level density reveals essential nuclear structure information such as thermodynamic properties and pair correlations as functions of temperature. These aspects of the molybdenum isotopes will be presented in a forthcoming work. Various applications of the Oslo method have been described in Refs. [17–21].

II. EXPERIMENTAL METHOD

The particle-γ coincidence experiments were carried out at the Oslo Cyclotron Laboratory for $^{93-98}$Mo using the CACTUS multidetector array. The charged ejectiles were detected with eight particle telescopes placed at an angle of 45° relative to the beam direction. An array of 28 NaI γ-ray detectors with

*Electronic address: magne.guttormsen@fys.uio.no

a total efficiency of ∼15% surrounded the target and particle detectors.

In the present work, results from eight different reactions on four different targets are discussed. Results from two of those reactions have been reported earlier. The beam energies for the different reactions are given in parentheses:

1. ^{94}Mo(^{3}He,$\alpha\gamma$)^{93}Mo (new, 30 MeV)
2. ^{94}Mo(^{3}He,^{3}He$'\gamma$)^{94}Mo (new, 30 MeV)
3. ^{96}Mo(^{3}He,$\alpha\gamma$)^{95}Mo (new, 30 MeV)
4. ^{96}Mo(^{3}He,^{3}He$'\gamma$)^{96}Mo (new, 30 MeV)
5. ^{97}Mo(^{3}He,$\alpha\gamma$)^{96}Mo (reported in [12,21], 45 MeV)
6. ^{97}Mo(^{3}He,^{3}He$'\gamma$)^{97}Mo (reported in [12,21], 45 MeV)
7. ^{98}Mo(^{3}He,$\alpha\gamma$)^{97}Mo (new, 45 MeV)
8. ^{98}Mo(^{3}He,^{3}He$'\gamma$)^{98}Mo (new, 45 MeV).

The targets were self-supporting metal foils enriched to ∼95% with thicknesses of ∼2 mg/cm^2 . The experiments were run with beam currents of ∼2 nA for 1–2 weeks. The reaction spin windows are typically $I \sim (2\text{–}6)\hbar$.

The experimental extraction procedure and the assumptions made are described in Refs. [14,16] and references therein. For each initial excitation energy E_i, determined from the ejectile energy and reaction Q value, γ-ray spectra are recorded. Then the spectra are unfolded using the known γ-ray response function of the CACTUS array [22]. These unfolded spectra are the basis for making the first-generation (or primary) γ-ray matrix [23], which is factorized according to the Brink-Axel hypothesis [4,24] as follows:

$$P(E_i, E_\gamma) \propto \rho(E_i - E_\gamma)\mathcal{T}(E_\gamma). \tag{1}$$

Here, ρ is the level density and $\mathcal{T}$ is the radiative transmission coefficient.

The ρ and $\mathcal{T}$ functions can be determined by an iterative procedure [16] through the adjustment of each data point of these two functions until a global χ^2 minimum of the fit to the experimental $P(E_i, E_\gamma)$ matrix is reached. It has been shown [16] that if one solution for the multiplicative functions ρ and $\mathcal{T}$ is known, one may construct an infinite number of other functions, which give identical fits to the P matrix by the following:

$$\tilde{\rho}(E_i - E_\gamma) = A \exp[\alpha(E_i - E_\gamma)]\, \rho(E_i - E_\gamma), \tag{2}$$

$$\tilde{\mathcal{T}}(E_\gamma) = B \exp(\alpha E_\gamma)\mathcal{T}(E_\gamma). \tag{3}$$

Consequently, neither the slope (α) nor the absolute values of the two functions (A and B) can be obtained through the fitting procedure.

The parameters A and α can be determined by normalizing the level density to the number of known discrete levels at low excitation energy [25] and to the level density estimated from neutron-resonance spacing data at the neutron binding energy S_n [26]. The procedure for extracting the total level density ρ from the resonance energy spacing D is described in Ref. [16]. Here, we will discuss only the determination of parameter B of Eq. (3), which gives the absolute normalization of $\mathcal{T}$. For this purpose we utilize experimental data on the average total radiative width of neutron resonances at S_n $\langle\Gamma_\gamma\rangle$.

We assume here that the γ decay in the continuum is dominated by $E1$ and $M1$ transitions. For initial spin I and parity π at S_n, the width can be written in terms of the transmission coefficient by the following [27]:

$$\langle\Gamma_\gamma\rangle = \frac{1}{2\rho(S_n, I, \pi)} \sum_{I_f} \int_0^{S_n} \mathrm{d}E_\gamma B\mathcal{T}(E_\gamma) \times \rho(S_n - E_\gamma, I_f), \tag{4}$$

where the summation and integration run over all final levels with spin I_f, which are accessible by γ radiation with energy E_γ and multipolarity $E1$ or $M1$.

A few considerations have to be made before B can be determined. Methodical difficulties in the primary γ-ray extraction prevents determination of the functions $\mathcal{T}(E_\gamma)$ in the interval $E_\gamma < 1$ MeV and $\rho(E)$ in the interval $E > S_n - 1$ MeV. In addition, $\mathcal{T}(E_\gamma)$ at the highest γ energies, above $E_\gamma \sim S_n - 1$ MeV, suffers from poor statistics. For the extrapolation of ρ we apply the back-shifted Fermi gas level density as demonstrated in Ref. [20]. For the extrapolations of $\mathcal{T}$ we use an exponential form. As a typical example, the extrapolations for ^{98}Mo are shown in Fig. 1. The contribution of the extrapolations of ρ and $\mathcal{T}$ to the calculated radiative width in Eq. (4) does not exceed 15% [18]. The experimental widths $\langle\Gamma_\gamma\rangle$ in Eq. (4) are listed in Table I. For ^{94}Mo, this width is unknown and is estimated by an extrapolation based on the ^{96}Mo and ^{98}Mo values.

The total radiative strength function for dipole radiation ($L = 1$) can be calculated from the normalized transmission coefficient $\mathcal{T}$ by the following:

$$f(E_\gamma) = \frac{1}{2\pi}\frac{\mathcal{T}(E_\gamma)}{E_\gamma^3}. \tag{5}$$

The RSFs extracted from the eight reactions are displayed in Fig. 2. As expected, the RSFs do not seem to show any odd-even mass differences. The results obtained for the (^{3}He,α) and (^{3}He,^{3}He$'$) reactions populating the same residual nucleus reveal very similar RSFs. Also for ^{96}Mo two different beam energies have been applied, giving very similar RSFs. Thus, the observed energy and reaction independency gives further confidence in the Oslo method.

III. DESCRIPTION OF THE RADIATIVE STRENGTH FUNCTIONS

An inspection of the experimental RSFs of Fig. 2 reveals that the RSFs are increasing functions of γ energy for $E_\gamma >$ 3 MeV. This indicates that the RSFs are influenced by the tails of the giant resonances. As follows from previous work, the main contribution (about 80%) is because of the electric dipole resonance (GEDR). The magnetic resonance (GMDR) and the isoscalar $E2$ resonance are also present in this region.

If the GEDR is described by a Lorentzian function, one will find that the strength function approaches zero in the limit $E_\gamma \to 0$. However, the ^{144}Nd(n,$\gamma\alpha$) reaction [29] strongly suggests that f_{E1} has a finite value in this limit. Kadmenskiĭ, Markushev, and Furman (KMF) have developed a model [30]

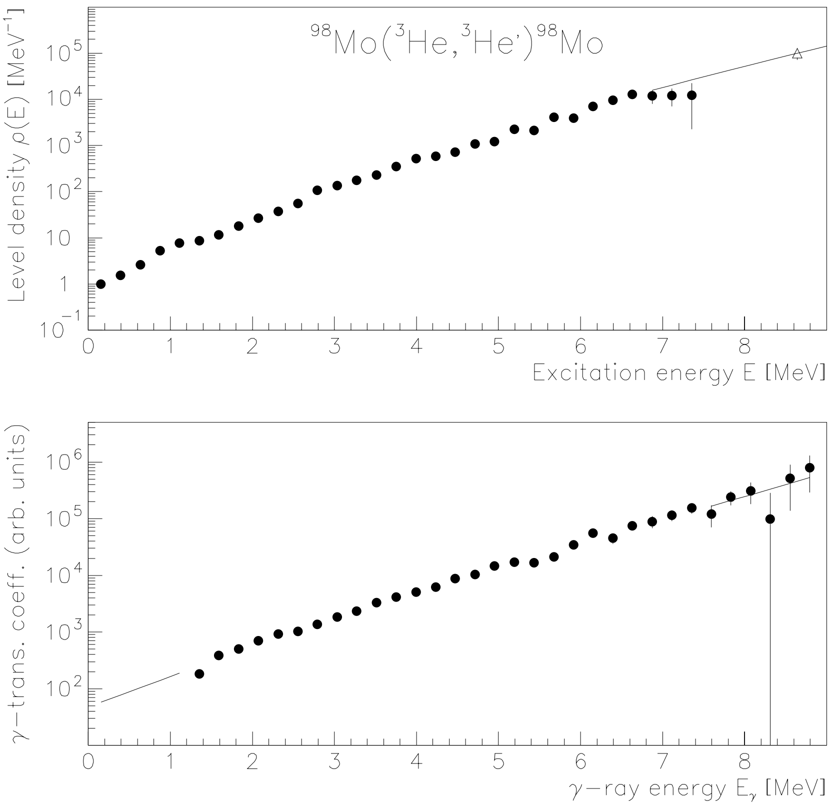

FIG. 1. Measured level density ρ (upper panel) and radiative transmission coefficient $\mathcal{T}$ (lower panel) for ^{98}Mo. The straight lines are extrapolations needed to calculate the normalization integral of Eq. (4). The triangle in the upper panel is based on resonance spacing data at S_n.

describing this feature for the electric dipole RSF:

$$f_{E1}(E_\gamma, T) = \frac{1}{3\pi^2\hbar^2c^2}\frac{0.7\sigma_{E1}\Gamma_{E1}^2\left(E_\gamma^2 + 4\pi^2T^2\right)}{E_{E1}\left(E_\gamma^2 - E_{E1}^2\right)^2}. \quad (6)$$

The temperature T depends on the final state f and for simplicity we adapt the schematic form

$$T(E_f) = \sqrt{U_f/a}, \quad (7)$$

where the level density parameter is parametrized as $a = 0.21A^{0.87}\,\mathrm{MeV}^{-1}$. The intrinsic energy is estimated by $U_f = E_f - C_1 - E_{\mathrm{pair}}$ with a back-shift parameter of $C_1 = -6.6A^{-0.32}$ MeV [31]. The pairing energy contribution E_{pair} is evaluated from the three-point mass formula of Ref. [33].

Although the KMF model has been developed for spherical nuclei, it has been successfully applied to ^{56,57}Fe and several rare earth nuclei [13,18–20] assuming a constant temperature parameter T in Eq. (6) (i.e., one that is independent of excitation energy). In this work we assume that the temperature depends on excitation energy according to Eq. (7), which gives an increase in the RSF at low γ energy [20].

The GMDR contribution to the total RSF is described by a Lorentzian. This approach is in accordance with numerous experimental data obtained so far [26]. However, the experimental data scatter and the resonance parameter values are uncertain. This is also true for the $E2$ resonance. The Lorentzian description of the $M1$ and $E2$ contributions are given in Ref. [17]. The resonance parameters for the $E1$, $M1$, and $E2$ resonances are taken from the compilations of Refs. [26,32] and are listed in Table I.

The enhanced RSF at low γ energies has at present no theoretical explanation. Recently, the same enhancement has

TABLE I. Parameters used for the radiative strength functions. The data are taken from Ref. [26]. The $E1$ resonance parameters for the even Mo isotopes are based on photo absorption experiments [32], and the parameters for the odd Mo isotopes are derived from interpolations.

Nucleus	E_{E1} (MeV)	σ_{E1} (mb)	Γ_{E1} (MeV)	E_{M1} (MeV)	σ_{M1} (mb)	Γ_{M1} (MeV)	E_{E2} (MeV)	σ_{E2} (mb)	Γ_{E2} (MeV)	$\langle\Gamma_\gamma\rangle$ (meV)
^{93}Mo	16.59	173.5	4.82	9.05	0.86	4.0	13.91	2.26	4.99	160(20)
^{94}Mo	16.36	185.0	5.50	9.02	1.26	4.0	13.86	2.24	4.98	170(40)[a]
^{95}Mo	16.28	185.0	5.76	8.99	1.38	4.0	13.81	2.22	4.97	135(20)
^{96}Mo	16.20	185.0	6.01	8.95	1.51	4.0	13.76	2.21	4.96	150(20)
^{97}Mo	16.00	187.0	5.98	8.92	1.58	4.0	13.71	2.19	4.95	110(15)
^{98}Mo	15.80	189.0	5.94	8.89	1.65	4.0	13.66	2.17	4.93	130(20)

[a]Estimated from systematics.

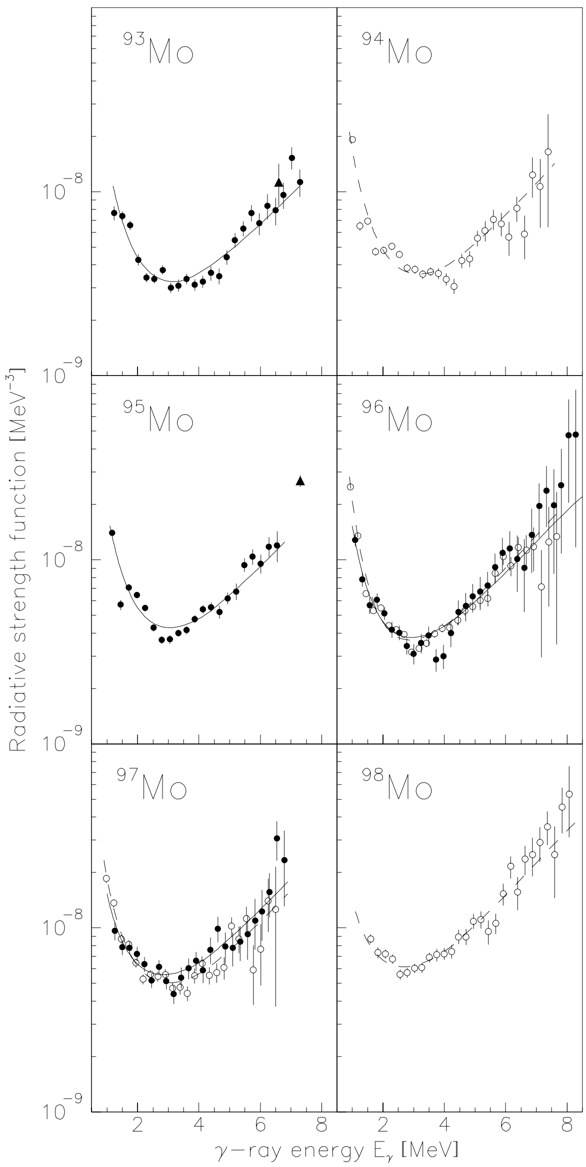

FIG. 2. Normalized RSFs for $^{93-98}$Mo. The filled and open circles represent data taken with the (^{3}He,α) and (^{3}He,^{3}He$'$) reactions, respectively. The filled triangles in ^{93,95}Mo are estimates of $E1$ RSF of hard primary γ rays [28] . The solid and dashed lines are fits to the RSF data from the two respective reactions (see text).

been observed in the iron isotopes [12,13]. We call this structure a soft pole in the RSF and choose a simple power law parametrization given by the following:

$$f_{\rm softpole} = \frac{1}{3\pi^2\hbar^2c^2}\mathcal{A}E_\gamma^{-b}, \tag{8}$$

where $\mathcal{A}$ and b are fit parameters and E_γ is given in MeV.

Previously, a pygmy resonance around $E_\gamma \sim 3$ MeV has been reported in several rare-earth nuclei [18–20]. The electromagnetic character of the corresponding RSF structure is now established to be of $M1$ type [9,10] and is interpreted as the scissors mode. Deformed nuclei can in principle possess this collective motion, and, for example, ^{98}Mo with a deformation of $\beta \sim 0.18$, could eventually show some reminiscence of the scissors mode. Data on ^{94}Mo [34] and ^{96}Mo [35] show a summed $M1$ strength to mixed symmetry 1^+ states around $\sim$3.2 MeV on the order of $\sim 0.6\mu_N^2$. This is about one order of magnitude lower than the $M1$ strength observed in well-deformed rare-earth nuclei using the present method. This $M1$ strength is deemed too weak to cause a visible bump in our RSFs above 3 MeV.

We conclude that a reasonable composition of the total RSF is as follows:

$$f = \kappa(f_{E1} + f_{M1} + f_{\rm softpole}) + E_\gamma^2 f_{E2}, \tag{9}$$

where κ is a normalization constant. Generally, its value deviates from unity for several reasons; the most important reasons are theoretical uncertainties in the KMF model and the evaluation of B in Eq. (4). We use κ, $\mathcal{A}$, and b as free parameters in the fitting procedure, and the results for the eight reactions are summarized in Table II.

In Fig. 3 the various contributions to the total RSF of ^{98}Mo are shown. The main components are the GEDR resonance and the unknown low-energy structure. We observe that the $E1$ component exhibits an increased yield for the lowest γ energies because of the increase in temperature T. However, this effect is not strong enough to explain the low-energy upbend.

Figure 2 shows the fit functions for all reactions and gives qualitative good agreements with the experimental data. The fitting parameters κ, $\mathcal{A}$, and b are all similar within the uncertainties. It should be noted that the soft pole parameters

TABLE II. Soft pole fitting parameters and integrated strenghts. The B values are only lower estimates (see text).

Reaction	κ	$\mathcal{A}$ (mb/MeV)	b	$B(E1\uparrow)$ (e^2 fm^2)	$B(M1\uparrow)$ (μ_N^2)	$B(E2\uparrow)$ ($10^3 e^2$ fm^4)
(^{3}He,α)^{93}Mo	0.44(4)	0.37(7)	2.6(3)	0.021(5)	1.9(4)	14(3)
(^{3}He,^{3}He$'$)^{94}Mo	0.36(2)	0.48(5)	2.5(2)	0.023(3)	2.1(3)	16(2)
(^{3}He,α)^{95}Mo	0.39(2)	0.48(6)	2.6(2)	0.024(4)	2.2(3)	16(2)
(^{3}He,^{3}He$'$)^{96}Mo	0.36(1)	0.60(4)	3.2(2)	0.022(2)	2.0(2)	16(1)
(^{3}He,α)^{96}Mo	0.32(4)	0.47(14)	2.7(6)	0.019(7)	1.7(6)	13(4)
(^{3}He,^{3}He$'$)^{97}Mo	0.38(3)	0.47(7)	2.4(3)	0.025(5)	2.3(4)	16(3)
(^{3}He,α)^{97}Mo	0.45(5)	0.30(10)	2.2(5)	0.020(8)	1.9(7)	13(5)
(^{3}He,^{3}He$'$)^{98}Mo	0.52(4)	0.22(7)	2.1(5)	0.018(7)	1.6(6)	12(4)

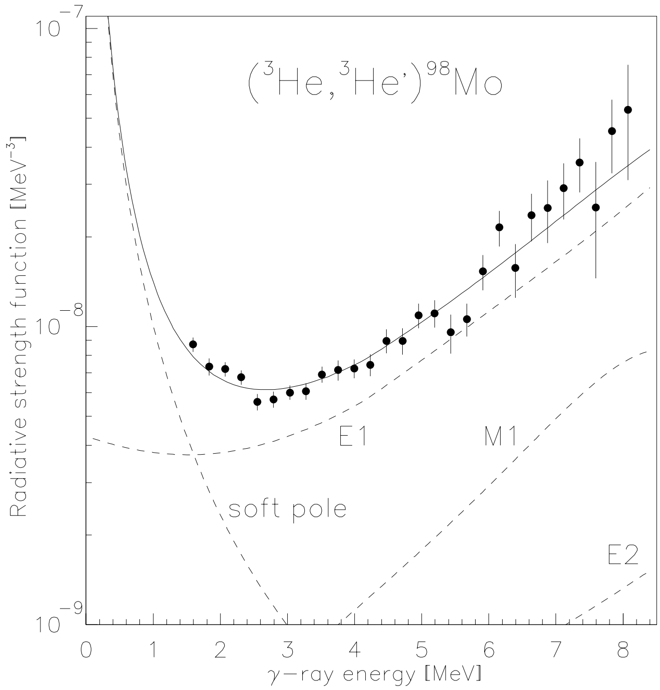

FIG. 3. Experimental radiative strength function of ^{98}Mo compared to a model description, including GEDR, GMDR, and the isoscalar $E2$ resonance. The empirical soft pole component is used to describe the low energy part of the RSF.

coincide with the description of the ^{57}Fe nucleus [13] having $\mathcal{A} = 0.47(7)$ mb/MeV and $b = 2.3(2)$.

The RSFs for $E_\gamma > 3$ MeV when going from $N = 51$ to 56 increase by almost a factor of 2 and this can be understood from the corresponding evolution of nuclear deformation. Following the onset of prolate deformation the GEDR will split into two parts, where 1/3 of its strength is shifted down in energy and 2/3 up. Photoneutron cross sections [32] show no splitting into two separate bumps; however, the observed increase in width Γ_{E1} as a function of neutron number (see Table I) supports the idea of a splitting, which is a well-known feature in other more deformed nuclei. Figure 2 demonstrates that the adopted widths describe very well the variation of the RSF strength as function of mass number.

To investigate whether the prominent soft pole structure is present in the whole excitation energy region, we have performed the following test. Assuming that the level density from Eq. (1) is correct, we can estimate the shape of the strength functions starting at various initial excitation energies using the following:

$$f(E_\gamma, E_i) = \frac{1}{2\pi}\frac{\mathcal{N}(E_i)P(E_i, E_\gamma)}{\rho(E_i - E_\gamma)E_\gamma^3}. \qquad (10)$$

Actually, $f(E_\gamma, E_f)$ would have been the proper expression to investigate, but because of technical reasons we chose $f(E_\gamma, E_i)$, which is equivalent to investigating $f(E_\gamma, E_f)$ because in our method E_f and E_i are uniquely related by $E_f = E_i - E_\gamma$. One problem is that the normalization

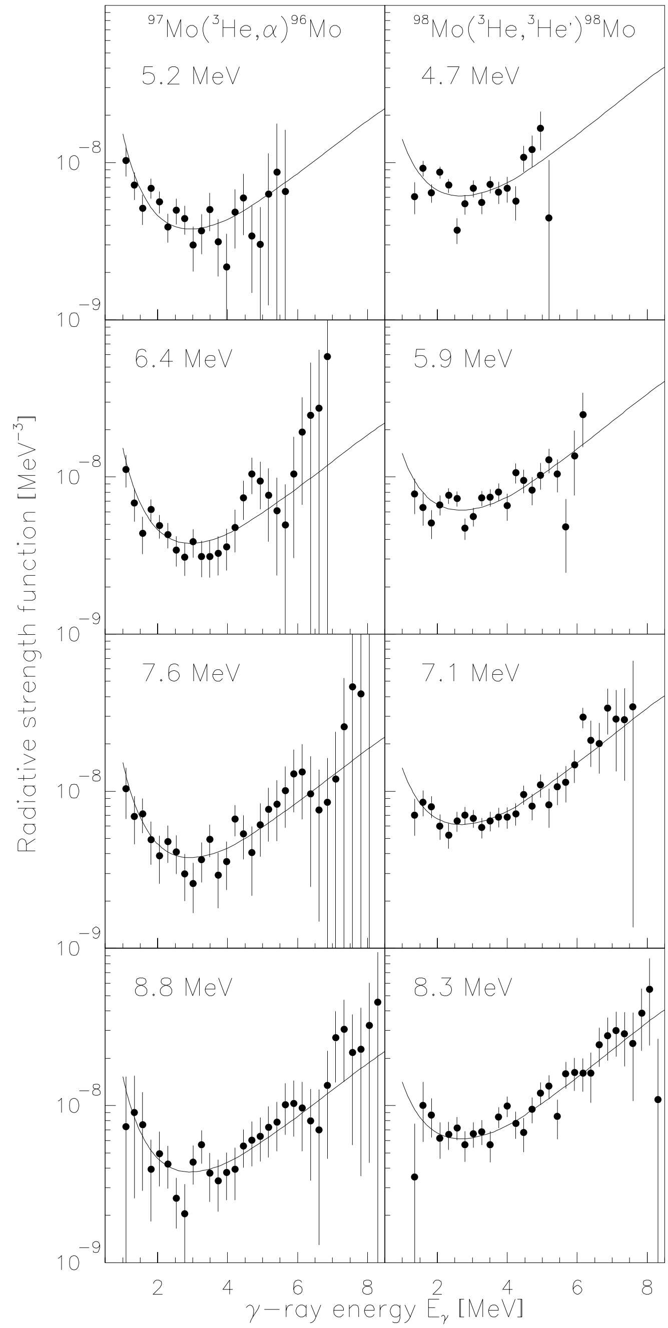

FIG. 4. RSFs for ^{96,98}Mo at various initial excitation energies. The soft pole is present for all E_i. The solid lines display the RSFs obtained in Fig. 2.

constant is only roughly known through the following estimate:

$$\mathcal{N}(E_i) = \frac{\int_0^{E_i} dE_\gamma \rho(E_i - E_\gamma)\mathcal{T}(E_\gamma)}{\int_0^{E_i} dE_\gamma P(E_i, E_\gamma)}, \qquad (11)$$

with $E_i < S_n$. However, for the expression $f(E_\gamma, E_i)$ we are interested only in the shape of the RSFs, and an exact normalization is therefore not crucial. The evaluation assumes that eventual temperature-dependent behavior of the RSF is small compared to the soft pole structure.[1]

In Fig. 4, the RSFs for ^{96,98}Mo are shown at various initial energies E_i. For comparison, the figure also includes the global RSFs (solid lines) obtained with the Oslo method (Fig. 2). Within the error bars the data support that the soft pole is present in all the excitation bins studied.

The origin of the soft pole cannot be explained by any known theoretical model. One would therefore need to know the γ-ray multipolarity as guidance for theoretical approaches to this phenomenon. Rough estimates of the reduced strength can be obtained from the following:

$$B(XL\uparrow) = \frac{1}{8\pi}\frac{L(2L+1)[(2L+1)!!]^2}{L+1}(\hbar c)^{2L+1} \times \int_{1\,\mathrm{MeV}}^{3\,\mathrm{MeV}} dE_\gamma f_{XL}(E_\gamma). \quad (12)$$

In the evaluation, we have integrated the soft pole between 1 and 3 MeV. Thus, the estimates listed in Table II for the reactions studied give only a lower limit for the respective $B(XL\uparrow)$ values. The correct result will of course depend on the functional form of $f_{\mathrm{softpole}}(E_\gamma)$ below 1 MeV; however, no experimental data exist in this region and any assumption here would be highly speculative. There seems to be no clear dependency of the B values on mass number or nuclear deformation.

With the assumptions above, we get in the case of an $E1$ soft pole an average $B(E1\uparrow)$ value of 0.02 e^2 fm^2, which is 0.07% of the sum rule for the GEDR. Assuming an $M1$ soft pole, we get roughly $B(M1\uparrow) \sim 2.0\mu_N^2$, which is 3–4 times larger than the observed strength to mixed symmetry 1^+ states around 3 MeV [34,35]. Provided the soft pole has $E2$ multipolarity we obtain finally a $B(E2\uparrow)$ value around 15000 e^2 fm^4, which is 5–15 times larger than the ones for the excitation to the first excited 2^+ states in the even molybdenum isotopes. Thus, we cannot exclude any of these multipolarities, since neither of them would yield unreasonably high transition strengths. Moreover, we would like to point out that the observed soft pole resides on top of the tails of giant resonances. Thus, the transition strength included in the soft pole has to be added to the strength in the giant resonance tail of the correct multipolarity to give the summed transition strength.

[1]Simulations using the KMF model with fixed temperature in the $T \sim 0.8$ MeV region indicate a maximum 20% effect from temperature dependence of the RSF.

IV. SUMMARY AND CONCLUSIONS

As expected, the observed RSFs reveal very similar shapes because they all refer to isotopes with the same nuclear charge. When going from $N = 51$ to 56 the RSF increases by almost a factor of two for $E_\gamma > 3$ MeV, which can be understood from the change of nuclear deformation. With the onset of deformation, the increasing resonance GEDR width Γ_{E1} is responsible for the increasing strength.

An enhanced strength at low γ energies is observed, which is equally strong for all isotopes and excitation energies studied. A similar enhancement has also been seen in the iron isotopes. The multipolarity of the soft pole radiation is unknown and there is still no theoretical explanation for this very interesting phenomenon.

ACKNOWLEDGMENTS

Financial support from the Norwegian Research Council (NFR) is gratefully acknowledged. Part of this work was performed under the auspices of the U.S. Department of Energy by the University of California, Lawrence Livermore National Laboratory, under Contract W-7405-ENG-48. A.V. E.A, U.A, and G.E.M acknowledge support from the National Nuclear Security Administration under the Stewardship Science Academic Alliances program through Department of Energy Research Grants DE-FG03-03-NA00074 and DE-FG03-03-NA00076 and U.S. Department of Energy Grant DE-FG02-97-ER41042.

[1] J. M. Blatt and V. F. Weisskopf, *Theoretical Nuclear Physics* (Wiley, New York, 1952).
[2] G. A. Bartholomew, I. Bergqvist, E. D. Earle, and A. J. Ferguson, Can. J. Phys. **48**, 687 (1970).
[3] G. A. Bartholomew, E. D. Earle, A. J. Ferguson, J. W. Knowles, and M. A. Lone, Adv. Nucl. Phys. **7**, 229 (1973).
[4] P. Axel, Phys. Rev. **126**, 671 (1962).
[5] S. Joly, D. M. Drake, and L. Nilsson, Phys. Rev. C **20**, 2072 (1979).
[6] M. Guttormsen, J. Rekstad, A. Henriquez, F. Ingebretsen, and T. F. Thorsteinsen, Phys. Rev. Lett. **52**, 102 (1984).
[7] M. Igashira, H. Kitazawa, M. Shimizu, H. Komano, and N. Yamamuro, Nucl. Phys. **A457**, 301 (1986).
[8] N. Ryezayeva, T. Hartmann, Y. Kalmykov, H. Lenske, P. von Neumann-Cosel, V. Yu. Ponomarev, A. Richter, A. Shevchenko, S. Volz, and J. Wambach, Phys. Rev. Lett. **89**, 272502 (2002).
[9] A. Schiller, A. Voinov, E. Algin, J. A. Becker, L. A. Bernstein, P. E. Garrett, M. Guttormsen, R. O. Nelson, J. Rekstad, and S. Siem, preprint, nucl-ex/0401038.
[10] M. Krtička, F. Bečvář, J. Honzátko, I. Tomandl, M. Heil, F. Käppeler, R. Reifarth, F. Voss, and K. Wisshak, Phys. Rev. Lett. **92**, 172501 (2004).
[11] N. Pietralla, P. von Brentano, R.-D. Herzberg, U. Kneissl, N. Lo Iudice, H. Maser, H. H. Pitz, and A. Zilges, Phys. Rev. C **58**, 184 (1998).
[12] E. Tavukcu, Ph.D. thesis, North Carolina State University, 2002.
[13] A. Voinov, E. Algin, U. Agvaanluvsan, T. Belgya, R. Chankova, M. Guttormsen, G. E. Mitchell, J. Rekstad, A. Schiller, and S. Siem, Phys. Rev. Lett. **93**, 142504 (2004).
[14] L. Henden, L. Bergholt, M. Guttormsen, J. Rekstad, and T. S. Tveter, Nucl. Phys. **A589**, 249 (1995).
[15] E. Melby, L. Bergholt, M. Guttormsen, M. Hjorth-Jensen, F. Ingebretsen, S. Messelt, J. Rekstad, A. Schiller,

S. Siem, and S. W. Ødegård, Phys. Rev. Lett. **83**, 3150 (1999).
[16] A. Schiller, L. Bergholt, M. Guttormsen, E. Melby, J. Rekstad, and S. Siem, Nucl. Instrum. Methods Phys. Res. A **447**, 498 (2000).
[17] U. Agvaanluvsan, *et al*., Phys. Rev. C **70**, 054611 (2004).
[18] A. Voinov, M. Guttormsen, E. Melby, J. Rekstad, A. Schiller, and S. Siem, Phys. Rev. C **63**, 044313 (2001).
[19] S. Siem, M. Guttormsen, K. Ingeberg, E. Melby, J. Rekstad, A. Schiller, and A. Voinov, Phys. Rev. C **65**, 044318 (2002).
[20] M. Guttormsen, A. Bagheri, R. Chankova, J. Rekstad, S. Siem, A. Schiller, and A. Voinov, Phys. Rev. C **68**, 064306 (2003).
[21] A. Schiller *et al*., Phys. Rev. C **68**, 054326 (2003).
[22] M. Guttormsen, T. S. Tveter, L. Bergholt, F. Ingebretsen, and J. Rekstad, Nucl. Instrum. Methods Phys. Res. A **374**, 371 (1996).
[23] M. Guttormsen, T. Ramsøy, and J. Rekstad, Nucl. Instrum. Methods Phys. Res. A **255**, 518 (1987).
[24] D. M. Brink, Ph.D. thesis, Oxford University, 1955.
[25] Data extracted using the NNDC On-Line Data Service from the ENSDF database.
[26] P. Obložinský, IAEA Report No. IAEA-TECDOC-1034, 1998.
[27] J. Kopecky and M. Uhl, Phys. Rev. C **41**, 1941 (1990).
[28] J. Kopecky and M. Uhl, in *Proceedings of a Specialists' Meeting on Measurement, Calculation and Evaluation of Photon Production Data, Bologna, Italy, 1994*, edited by C. Coceva, A. Mengoni, and A. Ventura [Report No. NEA/NSC/DOC(95)1], p. 119.
[29] Yu. P. Popov, in *Proceedings of the Europhysics Topical Conference, Smolenice, 1982*, edited by P. Obložinský (Institute of Physics, Bratislava, 1982), p. 121.
[30] S. G. Kadmenskiĭ, V. P. Markushev, and V. I. Furman, Yad. Fiz. **37**, 277 (1983) [Sov. J. Nucl. Phys. **37**, 165 (1983)].
[31] T. von Egidy, H. H. Schmidt, and A. N. Behkami, Nucl. Phys. **A481**, 189 (1988).
[32] Samuel S. Dietrich and Barry L. Berman, At. Data Nucl. Data Tables **38**, 199 (1988).
[33] J. Dobaczewski, P. Magierski, W. Nazarewicz, W. Satuła, and Z. Szymański, Phys. Rev. C **63**, 024308 (2001).
[34] C. Fransen *et al*., Phys. Rev. C **67**, 024307 (2003).
[35] C. Fransen *et al*., Phys. Rev. C **70**, 044317 (2004).